Photoreactivating Enzyme from *Escherichia coli*: Isolated Enzyme Lacks Absorption in Its Actinic Wavelength Region and Its Ribonucleic Acid Cofactor Is Partially Double Stranded When Associated with Apoprotein†

George D. Cimino‡ and John Clark Sutherland*

ABSTRACT: Isolated photoreactivating enzyme (PRE) from *Escherichia coli* exhibits some optical density at wavelengths greater than 300 nm. After correcting for the effects of light scattering, however, we find no true absorption in the spectral region that is required for enzymatic activity (320–450 nm). At shorter wavelengths, there is an absorption maximum near 260 nm that is due primarily to an RNA cofactor. Heating to 60 °C and subsequently cooling to 4 °C release the RNA cofactor from association with apoprotein and result in hyperchromicity. Circular dichroism indicates that the RNA associated with native enzyme is partially double stranded. At low ionic strength (μ = 0.01), heating to 15 °C or protease treatment at 4 °C results in irreversible loss of part of the double strandedness. We show that the difference spectrum at 4 °C between the absorption spectra of native enzyme and heat-treated enzyme can be fit by a superposition of reference spectra for denaturation of A-U and G-C base pairs derived from model polynucleotides. The coefficients of the linear combination of reference spectra were used to calculate the fraction of A-U and G-C base pairs. We find that both A-U and G-C base pairs are present in equal concentrations and that about 20% are in a double-stranded conformation in the native enzyme.

cis-syn-Cyclobutylpyrimidine dimers formed by ultraviolet irradiation of DNA ($\lambda < 320$ nm) are a major photoproduct with detrimental biological consequences. These lesions are responsible for cell death and mutation in procaryotes and have been implicated in the detrimental effects of ultraviolet radiation on eucaryotic systems (Setlow, 1966; Sutherland, B. M., et al., 1976; Hart et al., 1977). Dimers are formed between adjacent pyrimidines on the same DNA strand and result in a local denaturation at the damaged site in double-stranded DNA (Hayes et al., 1971). DNA photoreactivating enzymes (PRE)[1] (EC 4.1.99.3) restore biological integrity to ultraviolet-irradiated DNA by catalyzing the monomerization of pyrimidine dimers [for reviews, see Cook (1970), Rupert (1975), and Sutherland (1981)]. This catalysis requires recognition and binding of the enzyme to a dimer site in DNA. Monomerization occurs subsequent to binding but requires the absorption of photoreactivating light to break the cyclobutane ring of the pyrimidine dimer.

PRE from *Escherichia coli* uses light of wavelengths in the range 313–450 nm (Jagger et al., 1969; Sutherland et al., 1973) to bring about photoreactivation. Purified enzyme from *E. coli* consists of an apoprotein and an RNA cofactor (Snapka & Fuselier, 1977; Snapka & Sutherland, 1980). The absorption spectrum of this enzyme is dominated by the RNA with a maximum at 257 nm and a long tail of optical density extending to longer wavelengths (Sutherland et al., 1972; Wun et al., 1977; see below). Even though this trailing optical density extends through the wavelength region required for photoreactivation, no absorption peak is present coincident with the enzyme's action spectrum. Since the isolated enzyme is known to aggregate (Snapka & Fuselier, 1977), one might suspect that a large portion of the long-wavelength optical density originates from light scattering and not true absorption.

Wun et al. (1977) observed absorption changes upon binding of *E. coli* PRE to dimer-containing DNA. An absorption increase was found that has approximately the correct extinction and wavelength range to account for photoreactivation. Wun et al. (1977) suggested that the interaction of *E. coli* PRE with UV-DNA created a new absorption band. However, if a small absorption band between 300 and 450 nm is present in the enzyme alone, it is possible that it is hidden by the scattering effects and enhanced upon binding of the enzyme to its substrate. The increased absorption would then arise from enhancement of an existing band rather than the creation of an entirely new band. We now report that after correcting the absorption spectrum of isolated *E. coli* PRE for the effects of light scattering there is no significant absorbance beyond 320 nm.

An absorption decrease in the 260-nm region was also observed by Wun et al. (1977) upon binding of PRE to UV-DNA. Since the enzyme contains an RNA cofactor, this hypochromicity might indicate (1) a conformational change of the RNA within the enzyme, (2) a conformational change of the DNA bound to the enzyme, or (3) an interaction between the RNA of the RNA–apoprotein complex and the DNA. We therefore investigated the secondary structure of the RNA associated with *E. coli* PRE and the extent to which its structure is determined by protein association. Since the apoprotein is low in aromatic amino acids (Snapka & Sutherland, 1980) and apparently does not contain an additional chromophore responsible for its actinic absorption (present results), the spectroscopic properties of the enzyme at wavelengths greater than 240 nm are primarily due to the RNA cofactor. We investigated the secondary structure of the RNA

† From the Biology Department, Brookhaven National Laboratory, Upton, New York 11973. *Received March 18, 1982.* This research was supported by the U.S. Department of Energy and by Research Career Development Award CA00465 from the National Cancer Institute, Department of Health and Human Services, to J.C.S.

‡ Graduate Student from the Department of Molecular Biology and Biochemistry, University of California, Irvine, CA. Present address: Department of Chemistry, University of California, Berkeley, CA.

[1] Abbreviations: PRE, photoreactivating enzyme; CD, circular dichroism; nPRE, "native" PRE; dPRE, PRE inactivated by heating to 60 °C for 10 min and then cooling to 4 °C; UV, ultraviolet radiation; UV-DNA, UV-irradiated DNA; A-U, adenine–uracil base pair; G-C, guanine–cytosine base pair; TLC, thin-layer chromatography; Tris, tris(hydroxymethyl)aminomethane; EDTA, ethylenediaminetetraacetic acid; DTT, dithiothreitol.

0006-2960/82/0421-3914$01.25/0

in *E. coli* PRE by measuring absorption and circular dichroism (CD) changes induced by thermal denaturation and treatment with protease. Our results indicate the presence of double-stranded RNA in the holoenzyme that is stabilized by interactions with the apoprotein.

Materials and Methods

Photoreactivating enzyme was obtained from a strain of *E. coli* (W3350) lysogenic for phage λ carrying the phr gene (C1857S7dg D → J) (Sutherland et al., 1972). The enzyme was isolated according to the procedure reported by Snapka & Fuselier (1977) with one modification: isoelectric focusing was performed through a preformed pH gradient. The gradient was established by running the column for 48 h at 600 V without enzyme. The prefocused column was eluted and enzyme was added to the pH 7.2–6.5 region. After addition of enzyme, the column was run for 18 h at 400 V. A prefocused gradient reduces the time that the enzyme is subjected to electrofocusing. Protein content of the enzyme was determined by using the fluorescamine assay of Bohlen et al. (1973) with bovine serum albumin as a standard (ϵ_{1cm} = 6.6 at 280 nm). The ribonucleic acid cofactor was quantitated spectrophotometrically with an extinction coefficient of 8000 at 260 nm (Brownlee, 1972). This cofactor was separated from the holoenzyme by heat treatment at 60 °C for 10 min, followed by centrifugation at 15000*g* for 15 min. The supernatant was passed through a 0.2-μm filter (Millipore) before determination of the absorbance at 260 nm. This purification procedure yields an enzyme with a ratio of nucleic acid bases to PRE molecule of 12 ± 2.

Calf thymus DNA (Sigma Chemical Co., type I, D1501) was purified by phenol extraction. Dimers were formed in the DNA by exposure to 3×10^4 J/m^2 of 289-nm radiation in a Johns' monochromator (Johns & Rauth, 1965a,b). Samples were stirred during the irradiation and corrected for internal absorption (Johns et al., 1964). Fluence was monitored with a silicon photodiode (Model HUV-4000B, EG and G Inc., Salem, MA) that had been calibrated with malachite green actinometry (Fisher et al., 1967). The fraction of thymine converted to dimers was measured by the addition of a small amount of ^{3}H-labeled *E. coli* DNA before irradiation. After irradiation the DNA mixture was hydrolyzed, chromatographed on Polygram Cel 300 TLC plates (Macherey-Nagel, Duren, BRD; distributed by Brinkmann Instruments, Inc., Westbury, NY) with butanol–acetic acid–H_2O (80:12:30), and counted in a liquid scintillation counter (Sutherland et al., 1979). The percent thymine converted to dimers in the calf thymus DNA was determined by multiplying the measured dimer content of *E. coli* DNA by the factor (% A-T calf thymus/% A-T *E. coli*)^2 = 1.25 (Setlow & Carrier, 1966).

Photoreactivating enzyme activity was measured according to the method of Sutherland & Chamberlin (1973). Briefly, two samples of irradiated ^{32}P-labeled DNA are incubated with PRE; the control sample is maintained in the dark at 37 °C while the other sample is exposed to saturating levels of photoreactivating light in a circulating water bath maintained at 37 °C. The DNA in each sample is digested into inorganic phosphate, nucleosides, and small oligomers containing pyrimidine dimers. The digest is adsorbed to activated charcoal, filtered, and counted on a planchet counter. The difference between counts in the dark and light samples is a measure of enzyme activity. One unit of activity is that amount of enzyme monomerizing 1 pmol of pyrimidine dimers/h.

Protein digestion experiments were conducted with Pronase P (Sigma Chemical Co., type VI, no. P-5130). This nonspecific protease was incubated at 37 °C for 10 min before use to remove any contaminating RNase and DNase activities. A protease solution (0.02 mL) at 5 mg/mL was added to 2.5 mL of a PRE solution (0.15 mg/mL protein) in 10 mM Tris (pH 7.0)–0.1 mM EDTA. This mixture was maintained at 4 °C for 1 h before the CD measurements were performed.

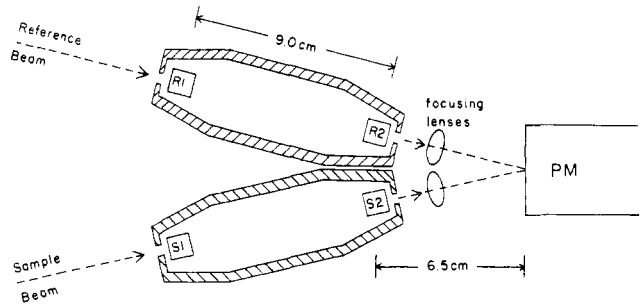

FIGURE 1: Plan view of alternate arrangements of the sample (S1 and S2) and reference cells (R1 and R2) within thermostated cuvette housings and their position with respect to the detector (PM).

Absorption and absorption difference spectra were recorded with a Cary 118C spectrophotometer (Varian Associates, Palo Alto, CA) fitted with temperature-regulated sample and reference cuvette holders (Models 1844100 and 1844200, respectively). Sample cuvettes were placed at either of two positions, S1 or S2, and reference cuvettes at either R1 or R2 (see Figure 1). The temperature of the cuvette holders was regulated with a Lauda circulator (Brinkmann Instruments, Inc., Westbury, NY). Sample and reference temperatures were monitored with type T thermocouples that were enclosed in glass capillaries and fitted into cuvette stoppers. The capillaries, inserted directly into the sample and reference solutions, were shaped so that they did not interfere with the optical beam. The cuvette compartment was purged with dry nitrogen gas to prevent condensation at low temperatures. A Tektronix 4051 computer controlled operation of the spectrophotometer and acquisition of data through the interface described by Sutherland & Boles (1978). The computer was also used to deconvolute the spectra according to eq 3 and 4 (vide infra).

CD spectra were recorded with an instrument that has been described elsewhere (Sutherland, J. C., et al., 1976). CD samples were housed in a water-jacketed holder and thermally regulated with a Lauda circulator. Sample temperature was monitored by the type of thermocouple probe described above. The sample compartment was continuously purged with dry nitrogen gas. The Tektronix 4051 also controlled operation of and data acquisition from this instrument.

Absorption spectra were corrected for the effects of light scattering by using two procedures. Both methods assume that the optical density due to scattering and the optical density due to absorption are additive, that is

$$OD1(\lambda) = A(\lambda) + S(\lambda) \quad (1)$$

where $A(\lambda)$ is the scatter-free absorption spectrum, $S(\lambda)$ is the spectrum of optical density due to scattered light, and $OD1(\lambda)$ is the measured optical density when the sample is in position S1 in Figure 1. The approach of Latimer & Eubanks (1962) requires measurement of two spectra in order to determine the true (i.e., scatter-free) absorption spectrum. These spectra are recorded at different sample-to-detector distances; in these experiments the two spectra were recorded with the sample in cuvette positions S1 and S2 as shown in Figure 1. The reference cuvette was placed in the corresponding position R1 or R2. We used these positions within the thermostated cuvette holder (rather than moving the sample to a position nearer the photomultiplier) because of

the necessity of keeping the enzyme at a low temperature where its activity is stable. With the sample in position S2 the optical density spectrum can be expressed as

$$OD2(\lambda) = A(\lambda) + \alpha S(\lambda) \quad (2)$$

Here, $A(\lambda)$ and $S(\lambda)$ have the same meaning as in eq 1 and α is a fractional coefficient that varies with the sample-to-detector distance and the scattering properties of the sample but which is found empirically to be independent of wavelength (Latimer & Eubanks, 1962). The value of α is given by the ratio $OD2(\lambda)/OD1(\lambda)$ at wavelengths where no absorption is present (e.g., $\lambda > 450$ nm). The true absorption spectrum is then obtained from

$$A(\lambda) = [OD2(\lambda) - \alpha OD1(\lambda)]/(1 - \alpha) \quad (3)$$

We also corrected to remove the effects of scattering with another empirical procedure described by Jagger (1967). The optical density in the absorption-free region ($\lambda > 450$ nm) was fitted to the equation $S(\lambda) = K\lambda^{-n}$, where K and n are constants whose values were determined by the method of least squares. The scatter-free absorption, $A(\lambda)$, for shorter wavelengths was obtained by subtracting the extrapolated scattering spectrum from the observed optical density, i.e.

$$A(\lambda) = OD(\lambda) - K\lambda^{-n} \quad (4)$$

This procedure and the procedure described by eq 3 gave essentially identical results.

Melting experiments were performed with both the CD instrument and the Cary 118C. Data were recorded when the thermocouple probe, inserted into the sample cuvette, registered the desired temperature. The rate of temperature change was 0.5 °C/min as suggested by Li (1978) for protein–nucleic acid complexes. Sample and reference solutions were purged with helium gas and overlaid with mineral oil prior to the start of an experiment to prevent formation of bubbles in the sample. Both the absorption and CD melting profiles were corrected for thermal expansion of the solvent. To correct the absorption melting profile for scattering changes as a function of temperature, we recorded complete spectra (500–240 nm) every 5 °C. The scattering contribution to the optical density at 260 nm was calculated by using the procedure of Jagger (1967). The scattering contribution at temperatures between each of the 5 °C increments was estimated by extrapolation between consecutive points. Data were smoothed and derivatives calculated according to the procedure of Savitzky & Golay (1964).

Results and Discussion

Absorption Spectrum and Enzymatic Activity. Absorption spectra of the purified *E. coli* PRE at 4 °C are shown in Figure 2. The spectrum labeled $OD1(\lambda)$ was recorded with the sample in cuvette position S1 and the reference cuvette containing buffer at R1 (see Figure 1). One large absorption peak is present at 257 nm due mainly to absorption by the RNA cofactor associated with the holoenzyme. This spectrum also contains a long, structureless tail extending to beyond 700 nm. A second absorption spectrum, $OD2(\lambda)$, was recorded with the sample in cuvette position S2 and the buffer blank at position R2. Spectrum $OD2(\lambda)$ is reduced in optical density at all wavelengths compared to spectrum $OD1(\lambda)$. As shown in the inset to Figure 2, the factor α is constant for all wavelengths greater than 320 nm and thus indicates that the sample's optical density in this wavelength region is due to scattering. If the majority of this optical density results from scattering effects, then the wavelength dependence of this optical density should be of the form λ^{-n}, where n is a constant.

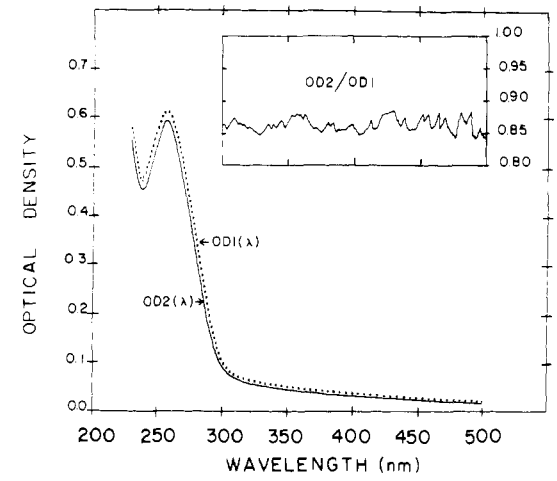

FIGURE 2: Absorption spectra of *E. coli* PRE (5.2×10^{-6} M) measured at two different sample-to-detector distances. $OD1(\lambda)$ (···) was recorded with the enzyme solution in cuvette position S1 and the reference buffer at R1; $OD2(\lambda)$ (—) was recorded with sample and reference solutions in cuvette positions S2 and R2, respectively. Spectra were taken at 4 °C in 0.01 M Tris-HCl buffer, pH 7.2, 0.1 mM EDTA, and 0.1 mM DTT. The wavelength scale is the same as shown at the bottom of the figure. The parameter α is the average value of the ratio of $OD1(\lambda)/OD2(\lambda)$ (inset) for the wavelengths shown.

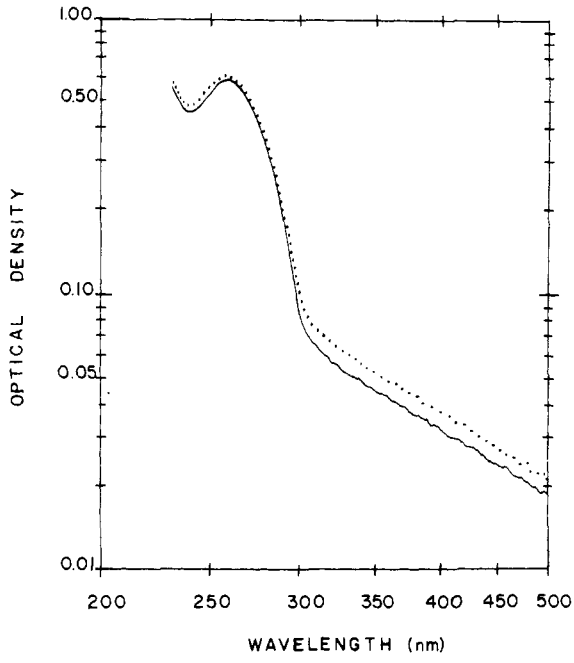

FIGURE 3: Plot of log $OD(\lambda)$ vs. log λ for spectra obtained with the sample of PRE in position 1 (···) and in position 2 (—).

Figure 3 is a plot of log $OD(\lambda)$ vs. log λ for spectra $OD1(\lambda)$ and $OD2(\lambda)$. Both spectra demonstrate linearity between log $OD(\lambda)$ and log λ at wavelengths greater than 320 nm. Hence, the optical density observed at wavelengths greater than 320 nm is not true absorption by *E. coli* PRE.

A scatter-corrected absorption spectrum of *E. coli* PRE obtained by use of eq 3 with a value of 0.86 for the parameter α is shown in Figure 4. To ensure that this result does not contain methodological artifacts, we also used the procedure described by eq 4 to obtain a scatter-corrected spectrum. Since photoreactivation by *E. coli* PRE does not occur at wavelengths greater than 450 nm (Sutherland et al., 1973), we fit the data of spectra $OD1(\lambda)$ and $OD2(\lambda)$ that extend beyond 450 nm to eq 4. The constants K and n, determined by the method of least squares, are given in Table I. The corre-

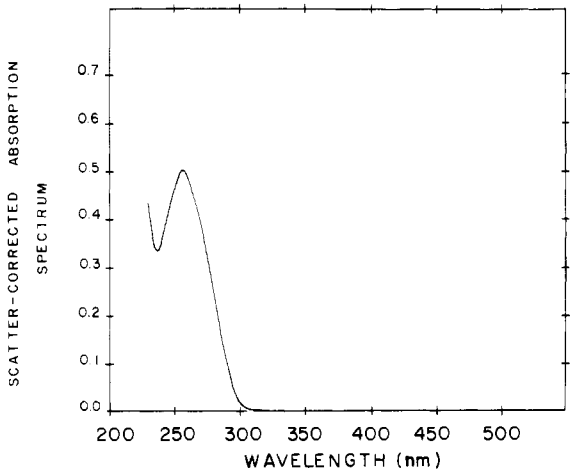

FIGURE 4: Scatter-corrected absorption spectrum of *E. coli* PRE obtained from spectra shown in Figure 2 by means of eq 3.

Table I: Scattering Parameters [$S(\lambda) = K\lambda^{-n}$] for Spectra OD1($\lambda$) and OD2($\lambda$)

spectrum	n	k
OD1(λ)	2.52	134 450
OD2(λ)	2.48	93 000

sponding scattering spectrum was subtracted from both OD1(λ) and OD2(λ). Using either OD1(λ) or OD2(λ), the method yields a scatter-corrected absorption spectrum of *E. coli* PRE that is indistinguishable from the spectrum obtained by the method of Latimer and Eubanks as shown in Figure 4.

From a comparison of Figures 2 and 4 the true absorbance at 260 nm is shown to be about 80% of the observed optical density. The long tail of optical density in the spectral region required for PRE activity is absent in the scatter-corrected spectrum. We estimate the root mean square uncertainty in the deconvoluted spectrum to be less than ±0.003 OD unit when using eq 3 and ±0.001 OD unit when using eq 4. The uncertainty is lower in the latter case since the random "noise" contained in OD1 is added to that of OD2 when the two spectra are subtracted in eq 3. The net noise is then magnified by division by the factor $1 - \alpha$. An uncertainty of 0.001 OD unit corresponds to a maximum extinction per mole of PRE of less than 190 M^{-1} cm^{-1} at wavelengths greater than 320 nm. Thus, *E. coli* PRE in the absence of irradiated DNA does not have a significant absorption band in its actinic wavelength region. Lack of absorbance by the *E. coli* PRE in the region between 320 and 450 nm might be explained in two ways. First, if the enzyme was inactivated during the absorption measurements one could postulate that inactivity was due to loss of the chromophore. On the other hand, if the lack of absorption is real, the chromophore must appear when the enzyme is complexed to its substrate. To distinguish between these possibilities, we divided the enzyme solution actually used to determine the spectra shown in Figures 2–4 into two fractions. One fraction was complexed to pyrimidine dimer containing DNA. The absorbance difference spectrum between the PRE–UV-DNA complex and the individual constituents of the complex is shown in Figure 5. The absorbance difference spectrum shows the presence of new absorption in the 295–450-nm region and hypochromicity below 295 nm, in agreement with the data of Wun et al. (1977). These absorption changes were not observed when *E. coli* PRE was mixed with unirradiated DNA. The second fraction of enzyme solution was assayed for in vitro photoreactivating activity.

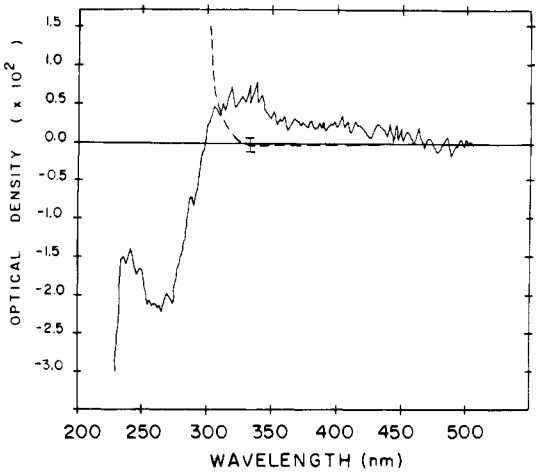

FIGURE 5: Absorption difference spectrum between PRE complexed to UV-DNA and the sum of isolated constituents. The PRE–UV-DNA complex was placed at cuvette position S2, the buffer at S1, UV-irradiated (15% thymine in dimers) calf thymus DNA (1.8×10^{-4} M) at R1, and PRE (5.2×10^{-6} M) at R2. The scatter-corrected absorption spectrum (- - -) of Figure 4 is shown for comparison. The error bar indicates the estimated uncertainty of the scatter-corrected absorption spectrum determined by the log–log extrapolation procedure (eq 4).

The enzyme solution had a specific activity of 1200 units/mg of protein after performing the absorption spectroscopy. Since it is possible to obtain enzyme solutions having twice this specific activity (Snapka & Sutherland, 1980), we estimate the maximal extinction for active, isolated molecules of PRE to be less than 380 M^{-1} cm^{-1} (i.e., twice the uncertainty of the absorption spectrum measurement, vide supra). This value is significantly less than the molar extinction coefficient of 6900 ± 1400 estimated by Wun et al. (1977) for the increased absorption at 350 nm.

We have thus shown that the hyperchromic peak between 300 and 450 nm is new absorption resulting from specific interaction between enzymatically active *E. coli* PRE and pyrimidine dimer containing DNA. Active enzyme does not possess the absorbance necessary for its catalytic activity. The chromophore responsible for photoreactivation by *E. coli* PRE is created only upon complex formation between PRE and its substrate, pyrimidine dimer containing DNA.

Spectroscopic Properties of RNA in E. coli PRE. The absence of a chromophore endogenous to *E. coli* PRE suggests that the spectroscopic properties of the enzyme in the 260-nm region may be due entirely to the aromatic amino acids of the apoprotein and the ribonucleic acid bases of the cofactor. From the amino acid composition of *E. coli* PRE (Snapka & Sutherland, 1980) the molar extinction coefficient due to the apoprotein at 260 nm is about 5170. Assuming an average of 12 RNA bases per PRE molecule and a molar extinction coefficient of 8000 per base, we find that greater than 94% of the absorption at 260 nm by *E. coli* PRE is due to nucleic acid absorption. Thus, the spectroscopic properties of *E. coli* PRE at wavelengths between 240 and 320 nm are predominantly those of the RNA cofactor.

The role of the RNA in *E. coli* PRE is unknown at present. P. Koka (personal communication) has isolated RNA in the size range of 10–15 bases from *E. coli* PRE. These data, along with the spectroscopic average of 12 ± 2 RNA bases per PRE, suggest that each enzyme molecule is associated with a single RNA oligonucleotide. Removal of the RNA by thermal dissociation (Snapka & Fuselier, 1977) or by adsorption to activated charcoal (Snapka & Sutherland, 1980) results in loss of enzymatic activity.

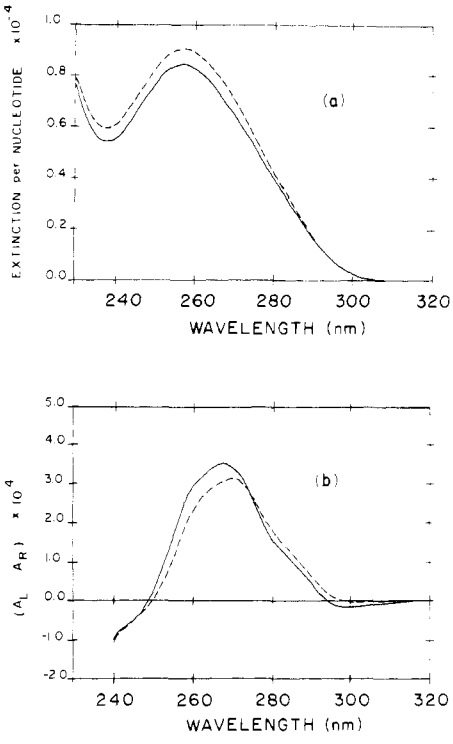

FIGURE 6: (a) Scatter-corrected absorption spectra of *E. coli* PRE before [nPRE (—)] and after [dPRE (---)] heating the enzyme to 60 °C for 10 min. Both spectra were recorded at 4 °C and are normalized to the absolute extinction per mole of nucleic acid. To estimate the absolute extinction, we compared scatter-corrected absorption spectra recorded at 4 °C to scatter-corrected spectra recorded at 90 °C (where no secondary structure exists). Both nPRE and dPRE have identical spectra at 90 °C. At 260 nm, the ratios of absorbance at 4 °C to that at 90 °C were used to calculate the absolute extinction. At 90 °C an extinction coefficient of 9600 was used for both samples. (b) Circular dichroism spectra of *E. coli* PRE before [nPRE (—)] and after [dPRE (---)] heating the enzyme to 60 °C for 10 min. Spectra were recorded at 4 °C. The enzyme solution was at a concentration of 4.2×10^{-6} M.

The absorption and CD spectra in Figure 6a,b show that the conformation of the RNA is irreversibly changed by heating the PRE to 60 °C for 10 min. All spectra were recorded at 4 °C and absorption spectra corrected for light scattering artifacts via eq 4. The enzyme that had been heated to 60 °C, which we designate as denatured PRE (dPRE), shows an increase in absorption and significant differences in CD compared to those of the native PRE (nPRE), which was kept at 4 °C. The increase in absorption suggests a decrease in the degree of base stacking, while the shift in the CD maximum from 265 to 270 nm and the disappearance of the negative CD band near 300 nm suggest a loss of base pairing (Hashizume & Imahori, 1967; Samejima et al., 1968; Borer et al., 1973). Using the analysis of Hashizume & Imahori (1967), we interpret the changes in the positive CD as indicating a shift in base stacking from 57% for nPRE to 44% for dPRE.

The hyperchromicity at 260 nm and the CD at 270 and 300 nm of the PRE as a function of temperature are shown in parts a and c of Figure 7; the derivative of the 260-nm absorption with respect to temperature is shown in Figure 7b. Total hyperchromicity is about 20%, but considerable structure is observed below 60 °C for both absorption and CD. The decrease in absorption near 15 °C, which is strikingly apparent in the negative values of the derivative spectrum in Figure 7b, suggests an increase in base stacking, possibly facilitated by the removal of some conformational constraint. The CD at both 270 and 300 nm also reflects this transition. Comparison

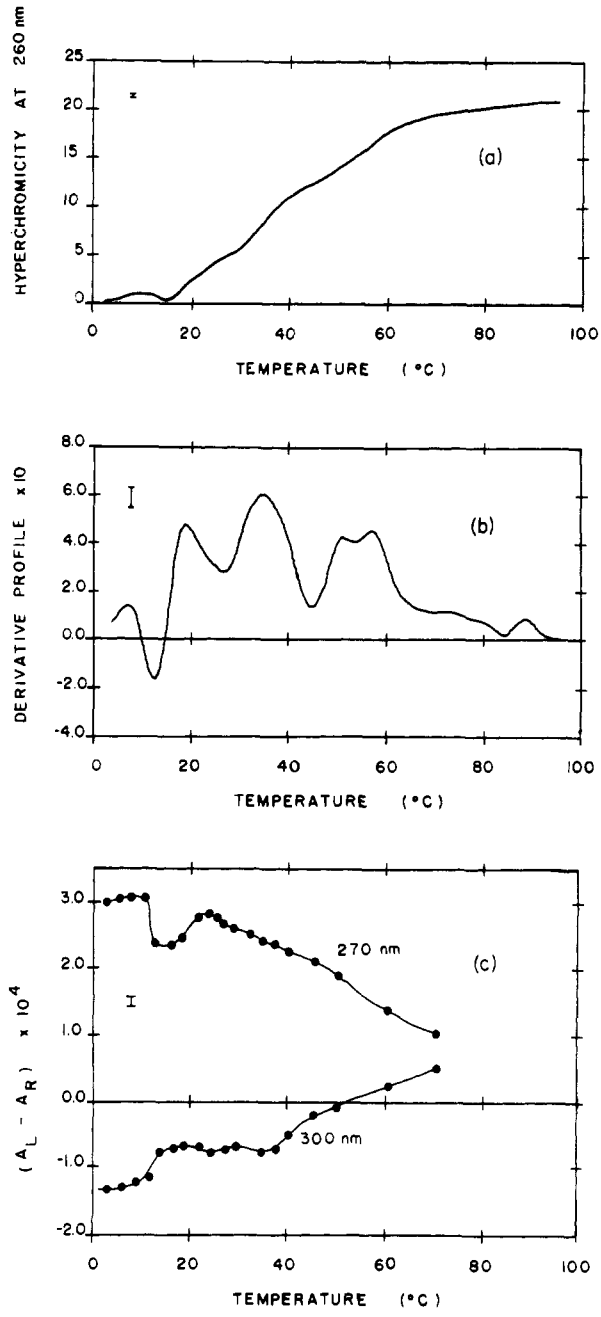

FIGURE 7: Melting profiles of *E. coli* PRE. Data are the average of two experiments on two different enzyme preparations. Resolution is indicated by error bars. (a) Absorption melting profile, corrected for thermal expansion and scattering changes; (b) derivative of absorption melting profile; (c) CD melting profile at 270 and 300 nm.

of the absorption and CD data suggests that a loss of base pairing facilitates an increase in base stacking. Presumably these effects are mediated via interactions of the RNA with the apoprotein. Additional evidence suggesting that the tertiary structure of the RNA is constrained by interactions with the apoprotein was obtained by treating native PRE with Pronase P for 1 h at 4 °C. The CD spectrum of this preparation was identical with the CD spectrum of the sample of PRE that had been denatured by heating to 60 °C for 10 min (data not shown). Heating native PRE to 35 °C causes loss of enzymatic activity and concomitant loss in double strandedness of the RNA as judged by loss of the negative CD at 300 nm (cf. Figure 7c). Comparison of the CD spectrum of native PRE recorded at 35 °C with the CD spectrum of PRE denatured by heating to 60 °C for 10 min (CD measured at

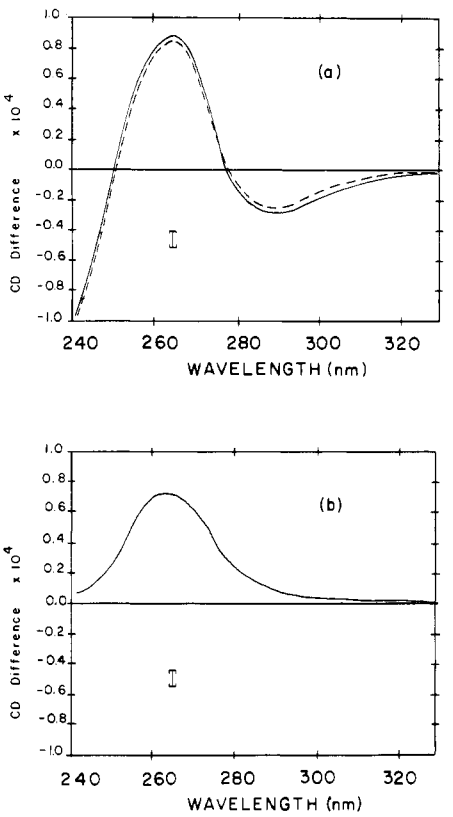

FIGURE 8: CD difference spectrum at 35 °C between native enzyme and heat-treated enzyme ($CD_{nPRE} - CD_{dPRE}$). Experimental uncertainty is indicated by error bars.

35 °C) shows no difference for wavelengths near 300 nm. However, the CD of the native PRE is still greater in the region near 260 nm as shown by the CD difference spectrum of Figure 8, thus indicating residual interactions between the RNA and apoprotein that remain after loss of the double strandedness of the RNA.

The composition of the base pairs involved in double-helical regions of polyribonucleotides (Cox, 1970) and polyribonucleoprotein complexes (Araco et al., 1975) can be estimated by analysis of absorption denaturation spectra. The difference spectrum of Figure 9a was obtained by subtracting the absorption spectrum of nPRE from the absorption spectrum of dPRE (cf. Figure 6a). Both absorption spectra were recorded at 4 °C and have been normalized to the absolute extinction per mole of nucleic acid present (10 bases per PRE molecule in this preparation). The experimental difference spectrum can be resolved by a superposition of the reference spectra for denaturation of A-U and G-C base pairs in double-helical polynucleotides according to

$$\Delta\epsilon_d = a\Delta\epsilon_{AU}(\lambda) + b\Delta\epsilon_{GC}(\lambda) \quad (5)$$

where $\Delta\epsilon_d$ is the observed difference spectrum between dPRE and nPRE, a and b are coefficients of the linear combination, and $\Delta\epsilon_{AU}(\lambda)$ and $\Delta\epsilon_{GC}(\lambda)$ are the reference spectra for the denaturation of A-U and G-C base pairs, respectively (Cox, 1970). The parameters $\Delta\epsilon_d$, $\Delta\epsilon_{AU}$, and $\Delta\epsilon_{GC}$ are expressed in units of liters per mole of nucleotide per centimeter. We used a least-squares analysis to fit the experimental data. The results, shown in Figure 9b, are for $a = 0.103 \pm 0.004$ and $b = 0.106 \pm 0.004$. This analysis demonstrates that the difference in absorption between nPRE and dPRE can be accounted for by the denaturation of equal numbers of A-U and G-C base pairs. Furthermore, since a and b represent the fraction of bases present that are involved in A-U and G-C base pairs, respectively, the total double-helical content of

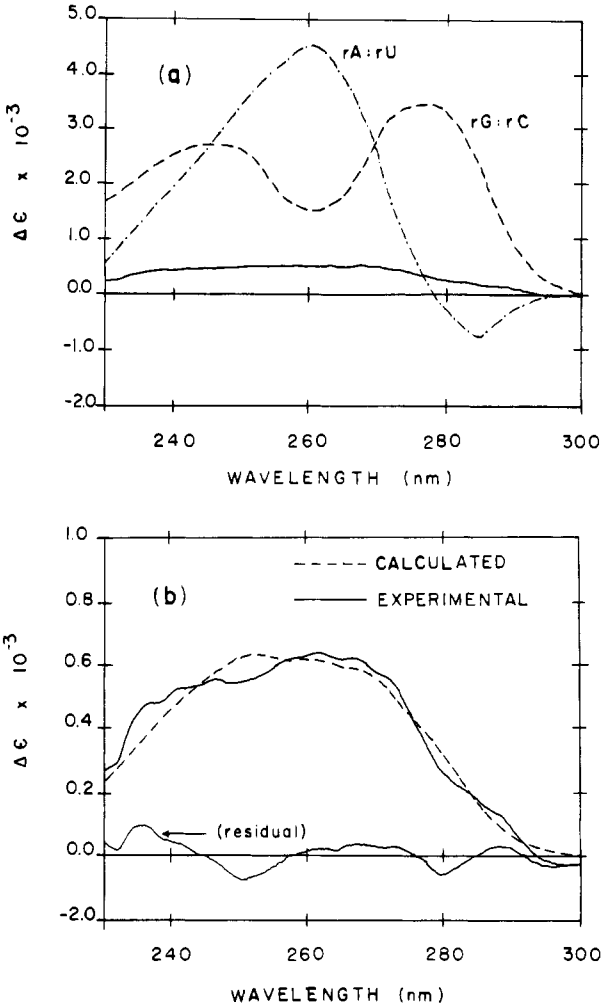

FIGURE 9: (a) Absorption difference at 4 °C (—) between nPRE and dPRE normalized to the absolute extinction per mole of nucleic acid. Also shown are the basis spectra [from Cox (1970)] for denaturation of A-U (-·-) and G-C (---) base pairs. (b) Experimental (—) absorption difference spectrum between nPRE and dPRE and calculated basis spectra for denaturation of A-U and G-C base pairs. The difference between these two spectra (residual) is also shown for comparison.

nPRE is 20.9 ± 0.8%. While the agreement between the calculated and experimental spectra shown in Figure 9b is obviously quite good, as with all such deconvolution procedures there is no absolute guarantee of the uniqueness of the solution.

The deconvolution results present an apparent dilemma in that we find 20% of the 10 bases are paired and at the same time we find an equal number of A-U and G-C pairs. A likely explanation is the distribution of base pairs among the enzyme molecules. From activity measurements we estimate that less than half of the isolated enzyme molecules are active. If the active molecules contain double-stranded RNA and the inactive molecules contain only single-stranded RNA, then the active molecules would have about two base pairs per molecule, but the entire population would have an average of only one base pair per RNA molecule as observed. A second possible explanation involves the accuracy assigned to the measured double-helical fraction. Absorption denaturation analysis is usually performed by comparing absorption profiles taken at two different temperatures: a low-temperature profile where secondary structure is stable is compared with a high-temperature profile where the secondary structure has melted away. This analysis is done on RNAs much larger than 10–15 bases in length and having a high degree of secondary structure so that end effects are minimized. Since the RNA associated

with *E. coli* PRE appears to be small, the end-effect problem was minimized by comparing absorption spectra of two forms of the same RNA taken at the same temperature. This approach might introduce some systematic error since it does not take into account stacking of single residues that become unpaired or stacking of residues that were unstacked because of constraints imposed by native secondary structure and protein association.

We have shown that enzymatically active *E. coli* photoreactivating enzyme in the absence of UV-DNA does not possess an absorption band in the spectral region coincident with its action spectrum. The absorption that is detected by absorption difference spectroscopy in the 295–450-nm region when the protein is mixed with UV-DNA is new absorption and not enhancement of a small, hidden absorption band. The nature of this new absorption is presently unknown. However, sensitized monomerization of isolated pyrimidine dimers in solution does occur in reactions mediated by photoexcited chemical sensitizers (Lamola, 1972, and references cited therein). Those sensitizers effective in monomerization either donate or accept electrons in the excited state. In these model studies, the sensitizer molecule is the absorber responsible for dimer breakage. Sutherland (1977) hypothesized that the repair of pyrimidine dimers by *E. coli* PRE is mediated through formation of a complex in which the absorption event results in a transfer of charge. This mechanism is consistent with the model studies and simultaneously explains the lack of an endogenous chromophore and the appearance of new absorption upon complex formation. Presumably, both protein and nucleic acid components are involved in the postulated charge-transfer complex.

Correcting the absorption spectrum of *E. coli* PRE for the effects of light scattering led to the observation that the RNA associated with native PRE is hypochromic with respect to the same RNA dissociated from the apoprotein. CD studies in the nucleic acid spectral region indicate that some of the RNA bases are in a double-stranded conformation that is stable at 4 °C in the native enzyme but absent after treating the enzyme with protease (at ionic strengths of both 0.01 and 0.18 M). CD data also indicate that some portion of the RNA is ordered to a greater extent when it is associated with native apoprotein. Thermal melting analysis of the nucleic acid has revealed that some segments of the RNA interact with the protein portion of *E. coli* PRE. This interaction occurs at temperatures as high as 35 °C. The melting data for the 15–25 °C region also suggest that the RNA is constrained to prevent base stacking when associated with the apoprotein.

Perturbation of base stacking by protein association is not novel. Interactions of RNA-binding proteins of the 30S ribosomal subunit with 16S RNA provoke dissociation of bound ethidium bromide, indicating a decrease of base stacking within the RNA–protein complex (Bollen et al., 1970). Interaction of calf thymus helix destabilizing protein with DNA (Kohwi-Shigematsu et al., 1978) and RNA (Karpel & Burchard, 1980) also decreases the extent of base stacking. From the absorption, CD, and melting data we conclude that a close physical interaction exists between the native apoprotein of *E. coli* PRE and at least some fraction of the RNA that purifies with the enzyme.

We have studied the conformation and conformational changes of the RNA associated with *E. coli* PRE in an attempt to investigate the origin of the hypochroism that appears when the enzyme binds to UV-DNA. Thermal denaturation analysis of this RNA indicates that several types of conformational rearrangements can occur. The rearrangement occurring between 18 and 25 °C results in absorption hypochromism and, if induced upon binding to UV-DNA, would contribute to the hypochromic effect observed by absorption difference spectroscopy. However, dimer sites in UV-DNA are known to be partially denatured (Hayes et al., 1971). Until the conformation of the DNA near a dimer site is known, it is difficult to assess the contribution by the UV-DNA to the hypochromic effect.

The thermal denaturation spectrum of the RNA is more complex than would be expected for an RNA 10–15 bases in length. 5S ribosomal RNA (which is about 120 nucleotides in length) has only a biphasic melting profile (Scott et al., 1968). Li (1978) has observed complicated melting profiles for histone-bound DNA. Different segments of DNA bound by less basic and more basic regions of histones were found to differ in melting temperatures by as much as 15 ° c. Similar regions of differential stabilization may be present in *E. coli* PRE and contribute to the complex melting profile of this RNA.

Acknowledgments

We thank Dr. B. M. Sutherland for the use of her laboratory facilities, generous supplies of *E. coli* PRE, and helpful discussions. We also thank Alice Shih and Kathleen Griffin for preparations of ^{32}P-labeled T7 DNA and ^{3}H-labeled *E. coli* DNA, respectively, and Dr. P. Borer, University of California at Irvine, for helpful discussions.

References

Araco, A., Belli, M., Giorgi, C., & Onori, G. (1975) *Nucleic Acids Res. 2*, 373–381.

Bohlen, P., Stein, S., Dairman, W., & Udenfriend, S. (1973) *Arch. Biochem. Biophys. 155*, 213–220.

Bollen, A., Herzog, A., Favre, A., Thibault, J., & Gros, F. (1970) *FEBS Lett. 11*, 49.

Borer, P. N., Uhlenbeck, O. C., Dengler, B., & Tinoco, I. (1973) *J. Mol. Biol. 80*, 759–771.

Brownlee, G. G. (1972) *Lab. Tech. Biochem. Mol. Biol. 3*, 22.

Cook, J. S. (1970) *Photophysiology 5*, 191–233.

Cox, R. A. (1970) *Biochem. J. 120*, 539–547.

Fisher, G. J., LeBlanc, J. C., & Johns, H. E. (1967) *Photochem. Photobiol. 6*, 757–767.

Hart, R. W., Setlow, R. B., & Woodhead, A. D. (1977) *Proc. Natl. Acad. Sci. U.S.A. 74*, 5574–5578.

Hashizume, H., & Imahori, K. (1967) *J. Biochem. (Tokyo) 61*, 738–749.

Hayes, F. N., Williams, D. L., Ratlift, R. L., Varghese, A. J., & Rupert, C. S. (1971) *J. Am. Chem. Soc. 93*, 4940–4952.

Jagger, J. (1967) *Introduction to Research in Photobiology*, Prentice-Hall, Englewood Cliffs, NJ.

Jagger, J., Stafford, R. S., & Snow, J. M. (1969) *Photochem. Photobiol. 10*, 383–395.

Johns, H. E., & Rauth, A. M. (1965a) *Photochem. Photobiol. 4*, 673–692.

Johns, H. E., & Rauth, A. M. (1965b) *Photochem. Photobiol. 4*, 693–707.

Johns, H. E., Pearson, M. L., LeBlanc, J. C., & Helleiner, C. W. (1964) *J. Mol. Biol. 9*, 503–524.

Karpel, R. L., & Burchard, A. C. (1980) *Biochemistry 19*, 4674–4682.

Kohwi-Shigematsu, T., Enomoto, T., Yamada, M., Nakanishi, M., & Tsuboi, M. (1978) *Proc. Natl. Acad. Sci. U.S.A. 75*, 4689–4693.

Lamola, A. A. (1972) *Mol. Photochem. 4*, 107–133.

Latimer, P., & Eubanks, C. A. H. (1962) *Arch. Biochem. Biophys. 98*, 274–284.
Li, H. J. (1978) *Methods Cell Biol. 18*, 385–396.
Rupert, C. S. (1975) in *Molecular Mechanisms for DNA Repair, Part A* (Hanawalt, P. C., & Setlow, J. K., Eds.) pp 73–87, Plenum Press, New York.
Samejima, T., Hashizume, H., Imahori, K., Fujii, I., & Miura, K. (1968) *J. Mol. Biol. 34*, 39–48.
Savitzky, A., & Golay, M. J. E. (1964) *Anal. Chem. 36*, 1627–1639.
Scott, J. R., Monier, R., Aubert, M., & Reynier, M. (1968) *Biochem. Biophys. Res. Commun. 33*, 794–800.
Setlow, J. K. (1966) *Curr. Top. Radiat. Res. 2*, 195–248.
Setlow, R. B., & Carrier, W. L. (1966) *J. Mol. Biol. 17*, 237–254.
Snapka, R. M., & Fuselier, C. O. (1977) *Photochem. Photobiol. 25*, 415–420.
Snapka, R. M., & Sutherland, B. M. (1980) *Biochemistry 19*, 4201–4208.
Sutherland, B. M. (1981) *Enzymes, 4th Ed. 14*, 481–515.
Sutherland, B. M., & Chamberlin, M. J. (1973) *Anal. Biochem. 53*, 163–176.
Sutherland, B. M., Court, D., & Chamberlin, M. J. (1972) *Virology 48*, 87–93.
Sutherland, B. M., Chamberlin, M. J., & Sutherland, J. C. (1973) *J. Biol. Chem. 248*, 4200–4205.
Sutherland, B. M., Oliver, R., Fuselier, C. O., & Sutherland, J. C. (1976) *Biochemistry 15*, 402–406.
Sutherland, J. C. (1977) *Photochem. Photobiol. 25*, 435–440.
Sutherland, J. C., & Boles, T. T. (1978) *Rev. Sci. Instrum. 49*, 853–854.
Sutherland, J. C., Cimino, G. D., & Lowe, J. T. (1976) *Rev. Sci. Instrum. 47*, 358–360.
Sutherland, J. C., Duval, J. F., Farland, W. H., & Griffin, K. P. (1979) *Photochem. Photobiol. 29*, 943–949.
Wun, K.-L., Gih, A., & Sutherland, J. C. (1977) *Biochemistry 16*, 921–924.

Specific Interaction of Anticodon Loop Residues with Yeast Phenylalanyl-tRNA Synthetase†

A. Gregory Bruce‡ and Olke C. Uhlenbeck*

ABSTRACT: Thirteen different yeast $tRNA^{Phe}$ variants with single nucleotide changes in positions 34–37 in the anticodon region were prepared by an enzymatic procedure described previously. Aminoacylation kinetics using purified yeast phenylalanyl-tRNA synthetase revealed that the level of aminoacylation was very different for different sequences inserted. The low level of aminoacylation was the result of a steady state between a slow forward reaction rate and spontaneous deacylation of the product. Aminoacylation kinetics performed at higher synthetase concentrations revealed that substitution at position 34 in $tRNA^{Phe}$ decreased the K_m nearly 10-fold but only had a small effect on V_{max}. Similar substitutions at positions 35, 36, and 37 had a lesser effect. These data suggest a sequence-specific contact between the anticodon of yeast $tRNA^{Phe}$ and the cognate synthetase.

In an early investigation on the interaction of yeast $tRNA^{Phe}$ with its cognate aminoacyl-tRNA synthetase, Thiebe et al. (1972) showed that the removal of four nucleotides (residues 34–37) from the anticodon loop of $tRNA^{Phe}$ did not completely destroy its ability to be aminoacylated. This experiment suggested that nucleotides in the anticodon loop were not involved in the specific protein–nucleic acid interaction. The view was supported by the data of Roe et al. (1973), who found that heterologous tRNAs with a variety of anticodon loop sequences could be aminoacylated by PRS.[1] Several other experiments, however, seemed to reach the opposite conclusion. By use of methods of fluorescence quenching (Krauss et al., 1973), oligonucleotide binding (Barrett et al., 1974), chemical modification with kethoxal (Litt & Greenspan, 1972), nuclease protection (Hörz & Zachau, 1973), and photochemical cross-linking (Ebel et al., 1979), the anticodon region was shown to interact with PRS.

Recently we have developed an enzymatic procedure which allows the removal of residues 34–37 from $tRNA^{Phe}$ and replacement of them with any arbitrary oligoribonucleotide (Bruce & Uhlenbeck, 1982). In preliminary experiments we noted that replacement of the $G_mpApApY$ sequence in $tRNA^{Phe}$ with ApApApC results in a tRNA which is much less active in the aminoacylation reaction. In this work we have prepared a series of tRNAs which systematically replace each of the four nucleotides and examine which positions are primarily responsible for the poor aminoacylation and therefore are presumably involved in the interaction with PRS.

Materials and Methods

Materials. Dinucleoside monophosphates and nucleoside 5′-diphosphates were purchased from Sigma Chemical Co. [5′-^{32}P]pCp was prepared from [γ-^{32}P]ATP (England et al., 1980) which was prepared from radioactive phosphate (Johnson & Walseth, 1978). L-[^{3}H]Phenylalanine (36.7 Ci/mmol) was purchased from Amersham. Yeast $tRNA^{Phe}$ was purchased from Boehringer-Mannheim (lot 1199234) and used directly for anticodon loop substitution or treated with tRNA nucleotidyltransferase and purified by gel electrophoresis for use in aminoacylation reactions.

† From the Department of Biochemistry, University of Illinois, Urbana, Illinois 61801. *Received November 20, 1981; revised manuscript received May 3, 1982.* This work was supported by a grant from the National Institutes of Health (GM 19059).

‡ Present address: Department of Biology, University of Utah, Salt Lake City, UT 84112.

[1] Abbreviations: $tRNA^{Phe}$, yeast phenylalanine-accepting tRNA; $tRNA^{Phe}_{AAAG}$, a $tRNA^{Phe}$ molecule which has ApApApG substituted for the anticodon loop nucleotides $G_mpApApY$ (positions 34–37); PRS, yeast phenylalanyl-tRNA synthetase; Tris, tris(hydroxymethyl)aminomethane; Hepes, 4-(2-hydroxyethyl)-1-piperazineethanesulfonic acid.

0006-2960/82/0421-3921$01.25/0